Near-field optical transducer for nanomechanical resonators

O. Basarir, S. Bramhavar, and K. L. Ekinci[a)]
College of Engineering and the Photonics Center, Boston University, Boston, Massachusetts 02215, USA

(Received 18 October 2010; accepted 27 November 2010; published online 23 December 2010)

We show that a single-mode tapered-fiber waveguide can be used as a sensitive transducer to couple to the motion of a nanomechanical resonator. When the waveguide and the resonator are sufficiently close to each other, small mechanical oscillations of the resonator can be actuated efficiently by the optical dipole force. Scattering of evanescent waves confined around the waveguide and the ensuing modulation in the optical transmission through the waveguide allow for sensitive detection of the resonator oscillations. Using this technique, we have measured high-frequency nanomechanical resonances with a ~ 150 fm $\mathrm{Hz}^{-1/2}$ noise floor at a detection power of ~ 100 μW. The tapered-fiber waveguide provides a single seamless transduction interface between the device chip and the measurement equipment, thus offering potential for use outside of the research laboratory. © *2010 American Institute of Physics*. [doi:10.1063/1.3530432]

Nanomechanical resonators, commonly referred to as nanoelectromechanical systems (NEMS), are expected to impact many future technologies, extending from biomedicine[1,2] to computation.[3] Yet, the development of NEMS-based nanotechnologies is still hindered by the difficulties in exciting and measuring the small NEMS motion. In the past decade, both optical[4–9] and electronic[10–13] phenomena have been exploited to actuate and sense nanomechanical motion. While impressive sensitivities have been reported, there has yet to emerge a versatile and simple transducer for NEMS—similar to the capacitive transducer for microelectromechanical systems. Typical NEMS transducers require complex experimental setups or delicate nanostructures or both. In electronic coupling, parasitic impedances typically impose limitations on signals and necessitate enhanced materials,[11] impedance matching,[12] or modulation techniques.[13] In the optical domain, alignment, positioning, and stability requirements along with the diffraction limit[7,9] pose challenges.

Near-field (evanescent) optical interactions provide an attractive avenue for nanomechanical motion transduction. Near-field interactions fit the length scale of NEMS well by retaining sensitivity beyond the diffraction limit. They can be used in noninterferometric approaches with less stringent coherence and stability requirements. Both actuation[4,6,14] and sensing[4–6,14–17] of motion can be realized based on near-field optical interactions. In this paper, we describe a simple, robust, and sensitive near-field interface in the form of a tapered-fiber waveguide for NEMS motion transduction. Our off-chip tapered-fiber waveguide provides a *seamless single-wire* interface between the NEMS chip and the measurement equipment, obviating the need for free-space optics.

In this approach, the displacement sensing mechanism is based on scattering of evanescent optical waves outside the waveguide. Optical dipole forces due to the field gradients around the waveguide allow for actuation of nanomechanical motion. Figure 1(a) shows an illustration of our single-mode tapered-fiber waveguide interface along with the block diagram of the measurement setup. The waveguide is positioned a distance z above a silicon doubly clamped beam resonator. The taper region is formed by heating and pulling a single-mode silica glass fiber[17] and has a diameter of $d \approx 1$ μm. Two different diode lasers are used in a pump-probe scheme. The light from the detection laser ($\lambda_p = 1580$ nm) passes through the taper, interacts with the NEMS resonator, and is sent onto a high-speed photodetector. Light from a second laser ($\lambda_d = 1530$ nm) is intensity-modulated and is also directed into the taper to actuate the resonator. A spectrum analyzer is used for noise measurements; a network analyzer is used to measure the driven response.

We first focus on detection of nanomechanical motion. Along the tapered-fiber waveguide, the optical mode becomes weakly guided. When a high-index dielectric such as silicon is present in the vicinity, the evanescent tail around the waveguide couples to the dielectric, reducing the transmission T through the waveguide. If there are small high-frequency oscillations in the gap between the dielectric and the waveguide, this will induce a modulation on the intensity of the transmitted light. By monitoring the high-frequency spectrum of the transmitted signal, mechanical motion can be detected. The optical power $P_{pd}(t)$ on the photodetector can be expressed as

$$P_{pd}(t) \approx P_{\mathrm{in}}\left[T(z_0) + \left| \frac{\partial T}{\partial z} \right|_{z_0} \sum_i \delta z_i(t) \right], \tag{1}$$

where P_{in} is the incident (probe) power on the waveguide. The derivative $|\partial T/\partial z|$ is evaluated at the static gap value $z = z_0$; $\delta z_i(t)$ correspond to the small time-dependent oscillations of the relevant modes of both the waveguide and the nanomechanical resonator.

Figure 1(b) shows the normalized dc transmission T through the tapered-fiber waveguide as it is slowly brought toward a 15 μm $\times$ 230 nm $\times$ 500 nm ($l \times t \times w$) doubly clamped nanomechanical beam using a calibrated positioning stage. When the NEMS-waveguide separation z is large, the optical power is directly transmitted to the photodetector. However, as z is decreased, T decreases exponentially until the waveguide snaps onto the NEMS at $z \approx 0$. The numerical z-derivative of the T curve is shown in the inset; the fit in the inset is an exponential. $|\partial T/\partial z|$ is the quantity which determines the displacement sensitivity (see below).

a)Electronic mail: ekinci@bu.edu.

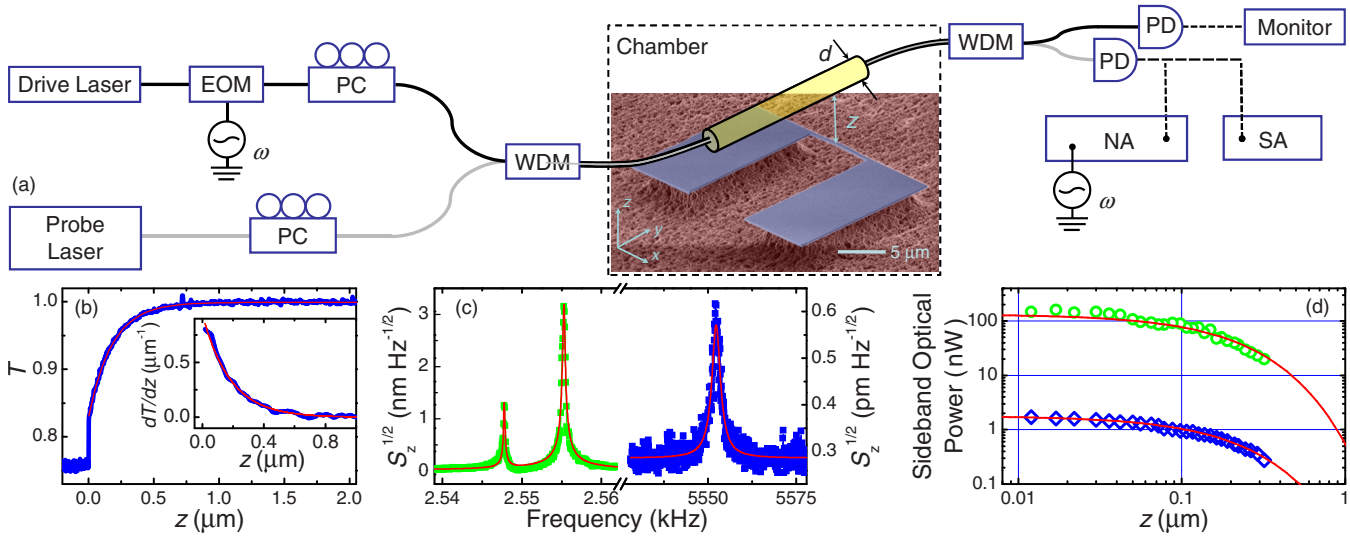

FIG. 1. (Color online) (a) Schematic of the experimental setup superimposed on the scanning electron microscopy image of a ($l \times t \times w = 15$ μm $\times 230$ nm $\times 500$ nm) doubly clamped beam. The transduction circuit comprises of an electro-optic intensity modulator, polarization controllers, wavelength division multiplexers, and photodetectors. The measurements are performed using a spectrum analyzer or a network analyzer. (b) Normalized transmission T and the numerical derivative $|\partial T/\partial z|$ (inset) as a function of z with theoretical exponential fits (solid lines). (c) Displacement noise spectral density $S_z^{1/2}(f)$ of the waveguide (left) and the NEMS resonator (right) measured in vacuum. (d) Integrated optical noise powers P_f^u (circles) and P_r (diamonds) vs z with exponential fits (solid lines).

Even when there are no external forces on the system, the thermomechanical motion of both the tapered-fiber waveguide and the NEMS will modulate the optical signal. Assuming that the waveguide and the resonator have well-defined thermal noise peaks at their respective resonance frequencies, the measured noise power will be prominent at the sidebands of these resonances. Indeed, the measured spectrum of the transmitted optical signal in Fig. 1(c) shows several noise peaks corresponding to the modes of the tapered-fiber waveguide and the doubly clamped beam. The measurement is performed in vacuum at a gap $z \approx 100$ nm with $P_{\text{in}} \approx 100$ μW. While the fundamental modes of the fiber are expected to be in orthogonal planes and degenerate in frequency, asymmetries in the taper structure result in two well-separated modes at $f_f^l \approx 2.548$ kHz and $f_f^u \approx 2.555$ kHz. Of these two, the mode at f_f^u moves mostly along the z direction and hence has the larger response. The high-frequency peak at $f_r \approx 5.55$ MHz corresponds to the fundamental out-of-plane mode of the doubly clamped beam.

$|\partial T/\partial z|$ and thermal noise measurements can provide a displacement calibration as well as the stiffnesses k_i of the mechanical modes in question. From Eq. (1), the noise powers P_f^u and P_r at the sidebands can be approximated as $P_{\text{in}}|\partial T/\partial z|_{z_0}\langle \delta z_i^2 \rangle^{1/2}$, where $\langle \delta z_i^2 \rangle^{1/2}$ is the rms thermal amplitude of the mode. Given that $\langle \delta z_i^2 \rangle^{1/2}$ is constant (temperature rise is estimated to be $\Delta\theta \leq 40$ μK), the noise power in each out-of-plane mode should closely follow $|\partial T/\partial z|$ when measured as a function of z. This is indeed the case for both the waveguide and the NEMS, as shown in Fig. 1(d). Here, the (integrated) noise power at f_f^u and f_r obtained from spectrum measurements is plotted as a function of z. Using the independently obtained $|\partial T/\partial z|$ from the inset of Fig. 1(b) and the experimental $P_{\text{in}} \approx 100$ μW value, we obtain $\langle \delta z_f^2 \rangle^{1/2} \approx 2.3$ nm and $\langle \delta z_r^2 \rangle^{1/2} \approx 31$ pm for the tapered-fiber waveguide and the nanomechanical resonator, respectively. The equipartition relation $\langle \delta z_i^2 \rangle = k_B\theta/k_i$, with θ being the temperature and k_B being the Boltzmann constant, then provides $k_f \approx 0.74 \times 10^{-3}$ N m^{-1} and $k_r \approx 4.1$ N m^{-1}. Using the extracted $\langle \delta z_f^2 \rangle$ and $\langle \delta z_r^2 \rangle$ values, one can readily convert measured signals into displacements, as done for the y-axis in Fig. 1(c). The displacement sensitivity (noise floor) is $S_z^{1/2} \approx 290$ fm Hz$^{-1/2}$ at $z = 100$ nm, further improving to $S_z^{1/2} \approx 150$ fm Hz$^{-1/2}$ at $z = 30$ nm.

We now consider the sensitivity of the displacement transducer as a function of the relevant NEMS size. Figure 2(a) shows T as a function of z measured as the waveguide was approached to silicon doubly clamped beams with identical lengths and thicknesses ($l \times t = 15$ μm $\times 230$ nm) but varying widths of $500 \leq w \leq 1500$ nm. At any given gap

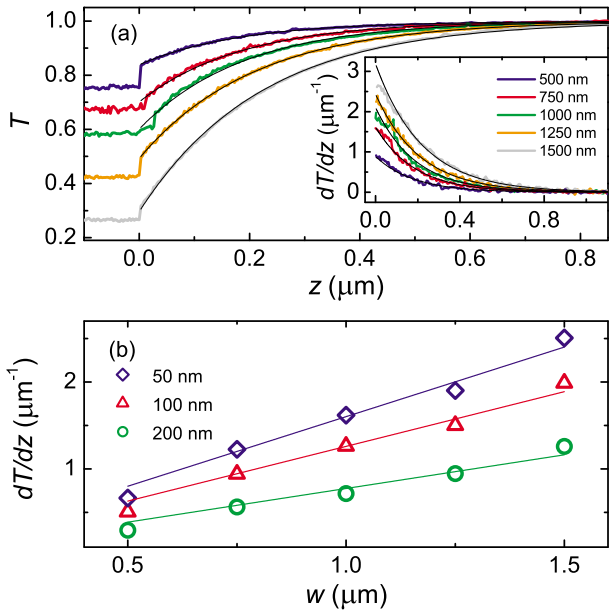

FIG. 2. (Color online) (a) T and $|\partial T/\partial z|$ (inset) vs z with exponential fits (solid black lines) for five doubly clamped beam resonators with different w. (b) $|\partial T/\partial z|$ as a function of w at fixed values of $z \approx 50$, 100, 200 nm. The solid lines are fits.

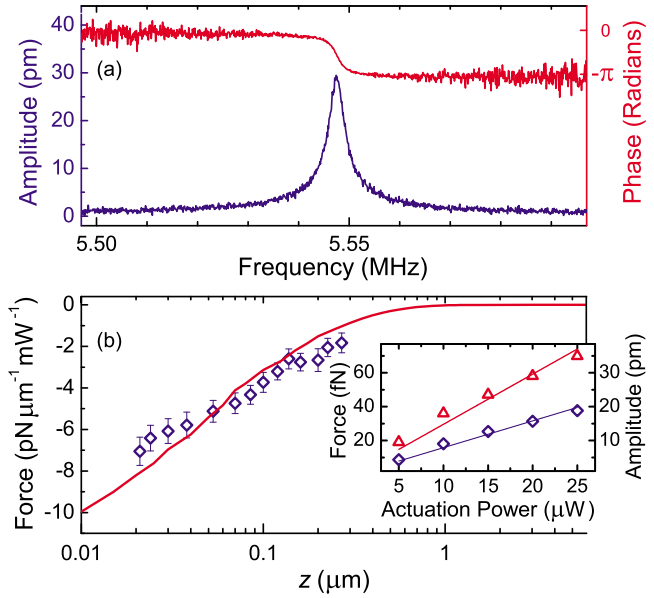

FIG. 3. (Color online) (a) Optically driven response of a ($l \times t \times w = 15\ \mu m \times 230\ nm \times 500\ nm$) doubly clamped beam. The response is measured at $z \approx 100$ nm with an actuation power of 25 μW and a probe power of 100 μW. (b) Normalized optical gradient force (normalized by interaction length w and actuation power) measured as a function of z. Open symbols are obtained from experiments, and the solid line is the result of FEM simulations. The inset displays the optical force as a function of actuation power. The force was obtained from measurements at $z \approx 50$ nm (triangles) and $z \approx 150$ nm (diamonds).

value z, the larger the device width, the smaller the transmission; this is consistent with the fact that the waveguide samples a larger dielectric area for a larger device width. $|\partial T/\partial z|$ vs z for each device is shown in the inset of Fig. 2(a). Figure 2(b) shows the dependence of $|\partial T/\partial z|$ on the device width w at three fixed gap values. A linear relationship is observed; $|\partial T/\partial z|$ and hence the displacement sensitivity increases with increasing w. For a given resonator, the displacement sensitivity increases as the device-waveguide gap is reduced.

Using the same interface, a second laser source can be used to resonantly excite devices through the optical gradient force. Figure 3(a) shows the optically excited response of the doubly clamped beam resonator of Fig. 1 detected by evanescent wave scattering at $z \approx 100$ nm. In a series of similar measurements shown in Fig. 3(b), we keep the actuation power fixed and measure the optical drive force (symbols) as a function of z. Force calibration is obtained by using the known displacement calibration and the k_r value. The solid line is calculated numerically[18] using two-dimensional finite-element-method (FEM) simulations. The complementary set of measurements in the inset shows the optical force versus the optical actuation power. Experimental data and theoretical calculations indicate a strong exponential dependence of the force on z and are in good agreement. We note that for the power levels used in this work, negligible power is dissipated in the resonator and $\Delta\theta \leq 40\ \mu$K. Hence thermal effects do not play a significant role in actuating the devices.[6]

Our transducer is insensitive to the phase of the light and can be implemented using an incoherent light source.[17] For further robustness, one could anchor the tapered-fiber waveguide to fabricated support structures on the device chip or flip-chip bond a separate waveguide chip[19] over the device chip. Even before such advances, our technique could be used in NEMS applications.

We acknowledge support from the NSF (through Grant Nos. ECCS-0643178, CBET-0755927, and CMMI-0970071) and the Boston University Photonics Center.

[1] A. K. Naik, M. S. Hanay, W. K. Hiebert, X. L. Feng, and M. L. Roukes, Nat. Nanotechnol. **4**, 445 (2009).
[2] P. S. Waggoner, M. Varshney, and H. G. Craighead, Lab Chip **9**, 3095 (2009).
[3] T.-H. Lee, S. Bhunia, and M. Mehregany, Science **329**, 1316 (2010).
[4] G. Anetsberger, O. Arcizet, Q. P. Unterreithmeier, R. Riviere, A. Schliesser, E. M. Weig, J. P. Kotthaus, and T. J. Kippenberg, Nat. Phys. **5**, 909 (2009).
[5] M. Eichenfield, R. Camacho, J. Chan, K. J. Vahala, and O. Painter, Nature (London) **459**, 550 (2009).
[6] M. Li, W. H. P. Pernice, C. Xiong, T. Baehr-Jones, M. Hochberg, and H. X. Tang, Nature (London) **456**, 480 (2008).
[7] T. Kouh, D. Karabacak, D. H. Kim, and K. L. Ekinci, Appl. Phys. Lett. **86**, 013106 (2005).
[8] A. Higo, S. Iwamoto, S. Ishida, Y. Arakawa, M. Tokushima, A. Gomyo, H. Yamada, H. Fujita, and H. Toshiyoshi, IEICE Electron. Express **3**, 39 (2006).
[9] N. Liu, F. Giesen, M. Belov, J. Losby, J. Moroz, A. E. Fraser, G. McKinnon, T. J. Clement, V. Sauer, W. K. Hiebert, and M. R. Freeman, Nat. Nanotechnol. **3**, 715 (2008).
[10] A. N. Cleland, J. S. Aldridge, D. C. Driscoll, and A. C. Gossard, Appl. Phys. Lett. **81**, 1699 (2002).
[11] S. C. Masmanidis, R. B. Karabalin, I. De Vlaminck, G. Borghs, M. R. Freeman, and M. Roukes, Science **317**, 780 (2007).
[12] U. Kemiktarak, T. Ndukum, K. C. Schwab, and K. L. Ekinci, Nature (London) **450**, 85 (2007).
[13] C. Chen, S. Rosenblatt, K. I. Bolotin, W. Kalb, P. Kim, I. Kymissis, H. L. Stormer, T. F. Heinz, and J. Hone, Nat. Nanotechnol. **4**, 861 (2009).
[14] J. Roels, I. De Vlaminck, L. Lagae, B. Maes, D. Van Thourhout, and R. Baets, Nat. Nanotechnol. **4**, 510 (2009).
[15] G. S. Wiederhecker, L. Chen, A. Gondarenko, and M. Lipson, Nature (London) **462**, 633 (2009).
[16] I. De Vlaminck, J. Roels, D. Taillaert, D. Van Thourhout, R. Baets, L. Lagae, and G. Borghs, Appl. Phys. Lett. **90**, 233116 (2007).
[17] O. Basarir, S. Bramhavar, G. Basilio-Sanchez, T. Morse, and K. L. Ekinci, Opt. Lett. **35**, 1792 (2010).
[18] M. L. Povinelli, M. Loncar, M. Ibanescu, E. J. Smythe, S. G. Johnson, F. Capasso, and J. D. Joannopoulos, Opt. Lett. **30**, 3042 (2005).
[19] M. C. M. Lee and M. C. Wu, Opt. Express **14**, 4703 (2006).